Bifurcation and Stability of Low-Order Steady Flows in Horizontally and Vertically Forced Convection

DAVID A. YOST

Martin Marietta Aerospace, Denver Division, Denver, CO 80201

HAMPTON N. SHIRER

Department of Meteorology, The Pennsylvania State University, University Park 16802

(Manuscript received 7 August 1980, in final form 8 October 1981)

ABSTRACT

The response of a convecting fluid to externally imposed horizontal and vertical temperature gradients is fundamentally different from that obtained when only vertical forcing is present. Using a three-component spectral model of two-dimensional shallow convection, we display the different forms and stability hierarchies of the stationary solutions as functions of both the vertical and the horizontal temperature differences. The structures of the possible steady states for zero and nonzero horizontal forcing are markedly different; the case of vertical heating only is singular and hence unobservable. Thus we demonstrate that the generic low-order convective model that most accurately reproduces some observations of Bénard convection, for example, must contain both horizontal and vertical heating parameters.

The steady behavior of the three-component model is described by three cusps in the thermal parameter plane for all values of domain aspect ratio and Prandtl number. Branching to periodic solutions occurs for all values of domain aspect ratio and Prandtl number. However, the qualitative nature of the sets of Hopf bifurcation points depends on the values of these parameters; three distinct types of Hopf bifurcation curves are identified. For some values of the horizontal and vertical heating, both thermally direct and indirect steady flows are stable and hence observable. The location of these cusps and Hopf bifurcation curves determines the regions of multiple equilibria and their stability. When the steady states lose stability via Hopf bifurcation, temporally periodic solutions exist nearby, and when all steady states are unstable, time-dependent flows must exist. This model also exhibits steady-state hysteresis and a mechanism whereby catastrophe, or sudden large change in the magnitude of the stationary solution, can occur.

1. Introduction

Two classes of convection have been studied extensively by fluid dynamicists. Each type represents atmospheric phenomena that usually are observed on widely different spatial and temporal scales. The first occurs when a viscous fluid is warmed from below; after the magnitude of the heating exceeds a critical value, the fluid begins to overturn (Chandrasekhar, 1961). This vertically forced, or Rayleigh, convection may serve, for example, as a model for cloud bands often found at the top of the planetary boundary layer (Kuettner, 1959, 1971).

The second kind of convection is driven by horizontal heating. When one wall of a rotating annulus is heated while the other wall is cooled, a two-dimensional cell in the radial-vertical plane develops (Fultz *et al.*, 1959). This type of flow is a prototype for the Hadley circulation found in the average large-scale meridional wind field of the tropical atmosphere; accordingly, we may call horizontally forced motion Hadley convection.

The above two varieties of convection can be viewed as special cases of motion in a fluid that is thermally forced in both the horizontal and the vertical. Indeed, neither purely Rayleigh nor purely Hadley solutions can be observed in any physical system because at least small temperature gradients in both directions are always present. In this article, we study a simple nonlinear spectral model of two-dimensional, shallow Boussinesq convection that responds to heating in both the horizontal and the vertical.

To develop our three-coefficient model, we employ the technique of maximum simplification of the equations in which the governing partial differential system is first converted to an infinite set of ordinary differential equations and then severely truncated to a small set that can be studied analytically (Lorenz, 1960, 1963). Small-scale contributions to the solutions evidently are lost by such a severe truncation, but important qualitative changes such as the number and types of transitions from one flow configuration to another can be studied in detail (Ogura and Yagihashi, 1970; McLaughlin and Martin, 1975;

0022-4928/82/010114-12$07.00
© 1982 American Meteorological Society

Unauthenticated | Downloaded 12/06/21 03:22 AM UTC

Vickroy and Dutton, 1979; Charney and Devore, 1979; Mitchell and Dutton, 1981). Although the relationship between the solutions of the ordinary and partial differential systems is not known, some truncated spectral models of two-dimensional shallow Boussinesq convection (Curry, 1978; Shirer and Dutton, 1979; Shirer, 1980) have been shown to exhibit a hierarchy of branching behavior analogous to that found by Krishnamurti (1970a,b), Fenstermacher *et al.* (1979) and Ahlers and Behringer (1978) in laboratory models of Bénard convection.

These truncated spectral models of Rayleigh convection in many ways adequately describe the qualitative nature of the bifurcations among the possible two-dimensional solutions, but Tavantzis *et al.* (1978) noted that the Rayleigh convection equations do not model well the transition from conductive to convective states; specifically, the observed magnitude of the circulation increases much more gradually than that predicted by the mathematical model. Tavantzis *et al.* (1978) suggest that any imposed horizontal temperature variations on the upper surface, which are likely present in laboratory experiments, will significantly affect the qualitative behavior of the branching convective solution. Thus, some bifurcative detail in the models of Lorenz (1963), McLaughlin and Martin (1975), Curry (1978), Shirer and Dutton (1979) or Shirer (1980) cannot be observed physically because the systems of equations contain only a vertical heating parameter. Nevertheless, the results of these studies certainly provide important guides for the development of more qualitatively correct models.

When a horizontal thermal forcing parameter is added to a set of spectral equations similar in form to that of Lorenz (1963), we will find that the resulting solutions model much better the observed transition from the conductive to the convective states as the magnitude of the lapse rate is varied. This corresponds to a prediction made by Shirer and Wells (1982), who have developed a technique for deciding when qualitatively important parameters have been excluded from a truncated spectral model. From their analysis they found that an inhomogeneous term, which can be introduced by horizontal heating, was necessary for the realistic description of the steady states.

Some of the truncated spectral systems cited above were used primarily to study the transitions from steady to temporal flows, and very complicated solutions were obtained in some cases. The periodic solutions found in some models usually branch from the steady states at Hopf bifurcation points. However, because these models lack a qualitatively important parameter for modeling of the steady states, the branching temporal ones cannot be represented properly. Indeed, the values of the Hopf bifurcation points in our model depend on the magnitudes of the horizontal as well as the vertical heating. These results suggest that the behavior of the temporal states may be affected significantly by the introduction of horizontal heating to the vertically forced model. Moreover, they demonstrate the prudence of first designing a model to be qualitatively correct in the simplest case (steady states) before a more time-consuming, expensive numerical study of the periodic solutions is begun. However, even this type of study must be undertaken with care, because no methods similar to that of Shirer and Wells (1982) yet exist for the determination of the necessary number of parameters for the adequate description of the temporal flows. This, however, is a long-range goal of our research.

The steady solutions to the three-component model form a cusp surface that also is found in catastrophe theory (Poston and Stewart, 1978). The two control parameters are the Rayleigh number Ra that represents the vertical forcing and the Hadley number Ha that measures the horizontal heating. Because of the orientation of the cusp surface, the model exhibits hysteresis as the sign of Ha is changed and circulation of fluid in either a clockwise or counterclockwise sense is predicted in some cases. This important result could be examined in a laboratory experiment.

2. Development of the spectral system

In this section we will derive the infinite system of nonlinear ordinary differential equations that subsequently will be truncated to yield our three-coefficient spectral model of horizontally and vertically heated convection. This development consists of three steps, in which we first obtain the approximate partial differential system and boundary conditions, then nondimensionalize the resulting set, and finally display the general spectral equations.

a. The boundary-value problem

We define the spatial domain of our problem by

$$R = \{(y, z) | 0 \leq y \leq \pi L,\ 0 \leq z \leq \pi H\}, \quad (2.1)$$

in which L and H are proportional to the width and the height of the rectangular region R.

We suppose that the convection can be represented by perturbation quantities superimposed on a reference state. This reference state is taken to be motionless, isothermal, isosteric and hydrostatic. Thus we have

$$\left.\begin{aligned} \mathbf{v}_0 = u_0\mathbf{i} + v_0\mathbf{j} + w_0\mathbf{k} = \nabla T_0 = \nabla \rho_0 = \mathbf{0} \\ \nabla p_0 = -g\rho_0\mathbf{k}, \end{aligned}\right\}, \quad (2.2)$$

in which $\mathbf{v}_0$ is the velocity vector, T_0 temperature, ρ_0 density and p_0 pressure; the gradient operator ∇ is

Unauthenticated | Downloaded 12/06/21 03:22 AM UTC

$$\nabla(\ ) = \mathbf{j}\frac{\partial}{\partial y}(\ ) + \mathbf{k}\frac{\partial}{\partial z}(\ ). \tag{2.3}$$

Denoting perturbation quantities by primes, we may write $T = T_0 + T'$, $p = p_{00} - \rho_0 gz + p'$ and $\rho = \rho_0 + \rho'$, in which we require that $|T'| \ll |T_0|$, $|p'| \ll |p_{00} - \rho_0 gz|$ and $|\rho'| \ll |\rho_0|$. Because the modeled convection is driven by heating on the container walls, we decompose T' further. We write T' as a sum of three terms, one depending on the time-independent, imposed horizontal temperature gradient $\Delta_y T$, one on the time-independent, imposed vertical temperature gradient $\Delta_z T$, and the third on the thermal response θ of the fluid to the imposed heating. The spectral expansion used later will require that the average of θ over the domain R remain zero. Thus we may write T' as

$$T'(y, z, t) = \frac{\Delta_y T}{\pi L} y + \frac{\Delta_z T}{\pi H} z + \theta(y, z, t). \tag{2.4}$$

The continuity equation $\nabla \cdot \mathbf{v} = 0$ is satisfied by a streamfunction ψ defined by

$$w = \partial\psi/\partial y, \quad v = -\partial\psi/\partial z. \tag{2.5}$$

With the use of (2.4) and (2.5) we may write the shallow Boussinesq equations as

$$\frac{\partial}{\partial t}\nabla^2\psi + K(\psi, \nabla^2\psi) = g\epsilon\frac{\partial\theta}{\partial y} + g\epsilon\frac{\Delta_y T}{\pi L} + \nu\nabla^4\psi, \tag{2.6}$$

$$\frac{\partial\theta}{\partial t} + K(\psi, \theta) + (\gamma_s - \gamma_e)\frac{\partial\psi}{\partial y} - \frac{\Delta_y T}{\pi L}\frac{\partial\psi}{\partial z} = \kappa\nabla^2\theta, \tag{2.7}$$

in which ∇^2 is the two-dimensional Laplacian operator and K is the Jacobian operator in the spatial variables y and z. In addition, γ_e is a lapse rate defined by

$$\gamma_e = -\Delta_z T/\pi H. \tag{2.8}$$

The lapse rate γ_s provides for isentropic temperature changes owing to pressure variations; in air $\gamma_s = \gamma_d$, the dry adiabatic lapse rate, but in water, γ_s is negligibly small (Dutton and Fichtl, 1969). The variables ν and κ are either the molecular or eddy values of the kinematic viscosity and the thermal diffusivity and ϵ is the isobaric coefficient of thermal expansion.

To complete the formulation of our boundary-value problem, we must specify for all times the magnitudes of ψ and θ on the sides of the domain R. We will assume that the boundaries are rigid so that the normal component of the velocity vanishes. Also, we assume that the boundaries are stress-free so that we have

$$\psi = \nabla^2\psi = 0, \tag{2.9}$$

everywhere on the perimeter of R for all times t.

The boundary conditions on θ are chosen so that a constant temperature difference in the horizontal and a constant heat flux in the vertical are maintained. These boundary conditions are the ones typically sought in experimental studies of horizontally and vertically forced convection. Thus, for all time t, we have

$$\left.\begin{aligned} \theta(0, z, t) = \theta(\pi L, z, t) = 0, \quad & 0 \leq z \leq \pi H \\ \frac{\partial\theta}{\partial z}(y, 0, t) = \frac{\partial\theta}{\partial z}(y, \pi H, t) = 0, \quad & 0 \leq y \leq \pi L \end{aligned}\right\}. \tag{2.10}$$

The basic model to be investigated here is stated as the boundary-value problem (2.6), (2.7), (2.9) and (2.10).

b. *The nondimensional system*

The qualitative dynamics for a wide range of physical systems are studied most conveniently when the external parameters are expressed in nondimensional form. In order to accomplish this, we use the definitions

$$\psi = \kappa\psi^*, \tag{2.11}$$

$$\theta = \frac{\kappa\nu}{g\epsilon H^3}\theta^*, \tag{2.12}$$

$$t = \frac{LH}{\kappa}t^*, \tag{2.13}$$

$$y = Ly^*, \tag{2.14}$$

$$z = Hz^*, \tag{2.15}$$

in which the asterisks denote nondimensional quantities.

With use of (2.11)–(2.15) in (2.6)–(2.7) we obtain the nondimensional system

$$\frac{\partial}{\partial t^*}\nabla^{*2}\psi^* + K^*(\psi^*, \nabla^{*2}\psi^*) = \sigma\frac{\partial\theta^*}{\partial y^*} - \mathrm{Ha} + \frac{\sigma}{A}\nabla^{*4}\psi^*, \tag{2.16}$$

$$\frac{\partial\theta^*}{\partial t^*} + K^*(\psi^*, \theta^*) = \mathrm{Ra}\frac{\partial\psi^*}{\partial y^*} - \frac{\mathrm{Ha}}{\sigma}\frac{\partial\psi^*}{\partial z^*} + \frac{1}{A}\nabla^{*2}\theta^*. \tag{2.17}$$

The Hadley number Ha and Rayleigh number Ra are the horizontal and vertical thermal forcing factors, respectively; they are given by

$$\mathrm{Ra} = g\epsilon(\gamma_e - \gamma_s)H^4/\nu\kappa, \tag{2.18}$$

$$\mathrm{Ha} = -g\epsilon\Delta_y T H^3/\pi\kappa^2, \tag{2.19}$$

in which γ_e is defined in (2.8). The Prandtl number

Unauthenticated | Downloaded 12/06/21 03:22 AM UTC

σ is

$$\sigma = \nu/\kappa \tag{2.20}$$

and we have introduced the aspect ratio

$$A = H/L. \tag{2.21}$$

For Ha $\neq 0$, the system (2.16)–(2.17) is nonhomogeneous, and, therefore, it does not admit of the trivial solution. This is consistent with Jeffreys theorem (Dutton, 1976), which states that the maintenance of a motionless state is forbidden whenever a nonzero temperature gradient is present on a level surface. But it also gives rise to our principal results. Convective flow as represented by the Bénard model cannot be observed; a perfectly motionless state cannot exist in a laboratory vessel because horizontal heating can never be completely eliminated.

The boundary conditions on the variables ψ^* and θ^* are identical to those on their dimensional counterparts as given in (2.9)–(2.10). We note, however, that the spatial domain R becomes the square

$$R^* = \{(y^*, z^*) | 0 \leq y^* \leq \pi, 0 \leq z^* \leq \pi\} \tag{2.22}$$

in the new coordinates.

c. *The spectral equations*

Fourier series representations for ψ^* and θ^* that satisfy the boundary conditions (2.9) and (2.10) are

$$\psi^* = (4/\pi^2) \sum_{j,k=1}^{\infty} \hat{\psi}_{jk} \sin(jy^*) \sin(kz^*), \tag{2.23}$$

$$\theta^* = (2/\pi^2) \sum_{j=1}^{\infty} \hat{\theta}_{j0} \sin(jy^*) + (4/\pi^2) \sum_{j,k=1}^{\infty} \hat{\theta}_{jk} \sin(jy^*) \cos(kz^*), \tag{2.24}$$

in which the Fourier coefficients, denoted by carets, are functions of time t^* only and the numerical constants are normalizing factors. The general system therefore is

$$-\lambda_{pq}\dot{\hat{\psi}}_{pq} = -\sum_{\substack{m,n=1 \\ r,s=1}}^{\infty} \lambda_{rs} D^{pq}_{mnrs} \hat{\psi}_{mn} \hat{\psi}_{rs} + \sigma \sum_{\substack{j=1 \\ k=0}}^{\infty} C_{pjqk} \hat{\theta}_{jk} - \mathrm{A}_{pq}\,\mathrm{Ha} + (\sigma/A)\lambda^2_{pq}\hat{\psi}_{pq}; \quad p, q = 1, 2, \ldots, \tag{2.25}$$

$$\dot{\hat{\theta}}_{pq} = -\sum_{\substack{m,n,r=1 \\ s=0}}^{\infty} E^{pq}_{mnrs} \hat{\psi}_{mn} \hat{\theta}_{rs} + \mathrm{Ra} \sum_{j,k=1}^{\infty} B_{pjkq} \hat{\psi}_{jk} - (\mathrm{Ha}/\sigma) q \hat{\psi}_{pq} - (\lambda_{pq}/A)\hat{\theta}_{pq}; \quad p = 1, 2, \ldots, \quad q = 0, 1, \ldots, \tag{2.26}$$

in which the overdot denotes differentiation with respect to t^*. For convenience, we have introduced a wavenumber parameter

$$\lambda_{pq} = (Ap)^2 + q^2. \tag{2.27}$$

The linear interaction coefficients A_{pq}, B_{pjkq}, C_{pjqk}, and the nonlinear interaction coefficients D^{pq}_{mnrs} and E^{pq}_{mnrs} are defined in the Appendix.

3. The minimum model

In the remainder of this article we will be concerned primarily with the distribution and local stability of the steady convective states as functions of the Rayleigh number Ra, which is proportional to the vertical temperature gradient, and the Hadley number Ha, which is proportional to the horizontal forcing. We study in detail an appropriate three-coefficient, or minimum, model in order to see what qualitatively different roles the two parameters play.

a. *The differential system*

There are three properties that a truncation of the spectral system (2.25)–(2.26) must have in order to be an adequate minimum model. It must be nonlinear, it should contain both thermal parameters Ra and Ha, and it must be impossible to truncate it further to a lower order set satisfying both of the first two conditions.

An analysis of the interaction coefficients (A1)–(A5) in the spectral system (2.25)–(2.26) shows both that a minimum model is composed of three equations and that there are an infinite number of possibilities. A representative minimum model is

$$-\lambda_{pq}\dot{\hat{\psi}}_{pq} = \sigma C_{pjqk}\hat{\theta}_{jk} - A_{pq}\,\mathrm{Ha} + (\sigma/A)\lambda^2_{pq}\hat{\psi}_{pq}, \tag{3.1}$$

$$\dot{\hat{\theta}}_{jk} = -E^{jk}_{pqrs}\hat{\psi}_{pq}\hat{\theta}_{rs} + \mathrm{Ra}B_{jpqk}\hat{\psi}_{pq} - (\lambda_{jk}/A)\hat{\theta}_{jk}, \tag{3.2}$$

$$\dot{\hat{\theta}}_{rs} = -E^{rs}_{pqjk}\hat{\psi}_{pq}\hat{\theta}_{jk} - (\mathrm{Ha}/\sigma)q\hat{\psi}_{pq}\delta_{rp}\delta_{sq} - (\lambda_{rs}/A)\hat{\theta}_{rs}, \tag{3.3}$$

in which r and s must satisfy at least one of the requirements

$$r = p + j, \quad s = q + k, \quad pk \neq qj, \tag{3.4}$$

$$r = \pm(p - j), \quad s = q + k, \tag{3.5}$$

$$r = p + j, \quad s = \pm(q - k), \tag{3.6}$$

$$r = \pm(p - j), \quad s = \pm(q - k), \quad pk \neq qj. \tag{3.7}$$

In order that $A_{pq} \neq 0$, we require that both p and q be odd. Hence, we must choose j and k even so that B_{jpqk} and C_{pjqk} do not vanish. We note that it is impossible to have Ha appear in (3.3) but not in (3.1). The set (3.1)–(3.3) is a general form of the Lorenz (1963) system, with the parameter Ha added. Fig. 1a depicts the $\hat{\psi}_{11}$ mode that we chose. With a direct circulation, the fluid rises at the warm boundary and sinks at the cool one. For later comparison, we show

Unauthenticated | Downloaded 12/06/21 03:22 AM UTC

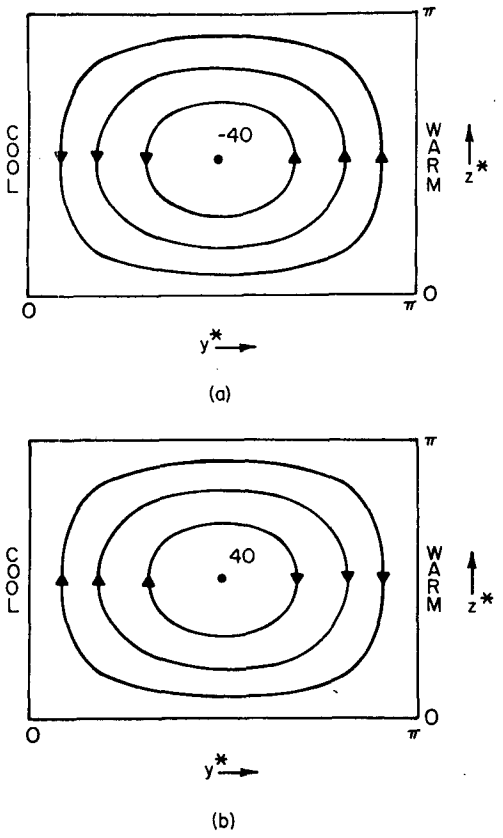

FIG. 1. Contours of the streamfunction field for the ψ_{11} normal mode showing thermally direct ($\dot{\psi}_{11} < 0$) flow (a) and thermally indirect ($\dot{\psi}_{11} > 0$) flow (b). Here Ha < 0 so that $\dot{\psi}_{11}$ Ha > 0 corresponds to thermally direct flow (a), and $\dot{\psi}_{11}$ Ha < 0 to thermally indirect flow (b).

an indirect circulation in Fig. 1b, which will appear in our results.

We note that in the case Ha = 0 Eqs. (3.1)–(3.3) exhibit a stationary bifurcation at a critical value R_c of the Rayleigh number Ra. To determine the appropriate values of p, q, j, k in (3.1)–(3.3) we assume that the first convective solution will branch from the trivial one at the minimum value of R_c. Here we find that R_c is given by

$$R_c = -\frac{\lambda_{pq}^2 \lambda_{jk}}{A^2 B_{jpqk} C_{pjqk}}, \tag{3.8}$$

in which A is the aspect ratio (2.21). Here B_{jpqk} and C_{pjqk} are the interaction coefficients (A2) and (A3) that have opposite signs. Thus $R_c > 0$, which corresponds to statically unstable stratifications. From (3.8), we note that the value of R_c is independent of the particular choices for r and s.

It can be shown that for $A \leqslant 1/\sqrt{2}$, R_c is a minimum with respect to p, q, j and k when $(p, q, j, k) = (2, 1, 1, 0)$, while for $A \geqslant 1/\sqrt{2}$, R_c is a minimum when $(p, q, j, k) = (1, 1, 2, 0)$. Therefore, since p must be odd in order that Ha be present in (3.1)–(3.3) we choose for our minimum model of horizontally and vertically forced convection the normal modes given by $(p, q, j, k) = (1, 1, 2, 0)$. Thus, the velocity field will be that of a single cell as depicted in Fig. 1.

From (3.4)–(3.7) we now see that there are two possibilities for the pair (r, s), $(r, s) = (1, 1)$ or $(r, s) = (3, 1)$. We arbitrarily choose the latter. We have found in our study that the particular choice of $\hat{\theta}_{rs}$ is apparently unimportant with respect to determining qualitative behavior. Thus, the minimum model of Hadley-Rayleigh convection is

$$-\lambda_{11}\dot{\psi}_{11} = \sigma C_{1210}\theta_{20} - A_{11}\,\mathrm{Ha} + (\sigma/A)\lambda_{11}^2\psi_{11}, \tag{3.9}$$

$$\dot{\theta}_{20} = -E^{20}_{1131}\psi_{11}\theta_{31} + \mathrm{Ra}B_{2110}\psi_{11} - (\lambda_{20}/A)\theta_{20}, \tag{3.10}$$

$$\dot{\theta}_{31} = -E^{31}_{1120}\psi_{11}\theta_{20} - (\lambda_{31}/A)\theta_{31}, \tag{3.11}$$

in which the circumflexes in (3.1)–(3.3) have been omitted.

b. Steady states

The stationary solutions of the minimum model are found by setting the right sides of (3.9)–(3.11) to zero. Upon substituting the definitions (A1)–(A5) for the interaction coefficients in (3.9)–(3.11), we find that the time-independent flow is given by

$$\theta_{20} = (\lambda_{11}^2\psi_{11}/A - 4\,\mathrm{Ha}/\sigma)/c, \tag{3.12}$$

$$\theta_{31} = A\psi_{11}(\lambda_{11}^2\psi_{11}/A - 4\,\mathrm{Ha}/\sigma)/(c\lambda_{31}) = A\psi_{11}\theta_{20}/\lambda_{31}, \tag{3.13}$$

$$\lambda_{11}^2\psi_{11}^3 - 4h\psi_{11}^2 + 8\lambda_{11}^2\lambda_{31}(1 - r)\psi_{11} - 32h\lambda_{31} = 0, \tag{3.14}$$

in which h is a modified Hadley number defined by

$$h = \frac{A\,\mathrm{Ha}}{\sigma}, \tag{3.15}$$

r is defined by

$$r = \frac{128\,\mathrm{Ra}}{9\pi^4\lambda_{11}^2} = \frac{\mathrm{Ra}}{R_c}, \tag{3.16}$$

and $c = 16/3\pi^2$.

It is convenient to first consider the two special cases of heating in only one direction. When Ha = 0, two nontrivial convective states given for $r \geqslant 1$ by

$$\psi_{11} = \pm[8\lambda_{31}(r - 1)]^{1/2}, \tag{3.17}$$

branch from the conductive one at $r = 1$ (Fig. 2). In Fig. 2, the linearly stable solutions are denoted by the heavier lines. Also, in agreement with Lorenz (1963), the nontrivial solutions lose stability at $r = r_h$ via a Hopf bifurcation.

Primitive Hadley flow differs radically from primitive Rayleigh convection. It can be shown that the only steady solution to (3.9)–(3.11) for $r = 0$ is given

Unauthenticated | Downloaded 12/06/21 03:22 AM UTC

by $\theta_{20} = \theta_{31} = 0$ and

$$\psi_{11} = 4A\,\mathrm{Ha}/\sigma\lambda_{11}^2 . \qquad (3.18)$$

Thus, we find that the magnitude of the unique, steady, single-cell circulation varies linearly with the horizontal forcing and that it is thermally direct (Fig. 1a).

Moreover, the flow of the minimum model for $r = 0$ is governed by a Liapunov function V. After the linear transformation $\psi = \psi_{11} - 4A\,\mathrm{Ha}/\sigma\lambda_{11}^2$ that situates the steady solution (3.18) at the origin of phase space, V takes the form

$$V(\psi, \theta_{20}, \theta_{31}) = \frac{\lambda_{11}^3}{c^2\sigma}\psi^2 + \frac{\theta_{20}^2}{16} + \frac{\theta_{31}^2}{32}, \qquad (3.19)$$

for it can be shown that $\dot{V} \leqslant 0$ everywhere and $\dot{V} < 0$ somewhere on any nontrivial orbit. Then it follows that (3.18) is globally asymptotically stable (Hirsch and Smale, 1974) and all trajectories tend to the origin as time increases.

Also if $|r|$ is sufficiently small, then we expect that a quadratic Liapunov function will still exist and that the unique stationary solution (Fig. 3) will be a global attractor. Because this result does not depend on a singular choice for r, we believe that the observed convective motion will resemble the primitive Hadley flow when the vertical stratification is weak.

The set of points in the thermal parameter plane

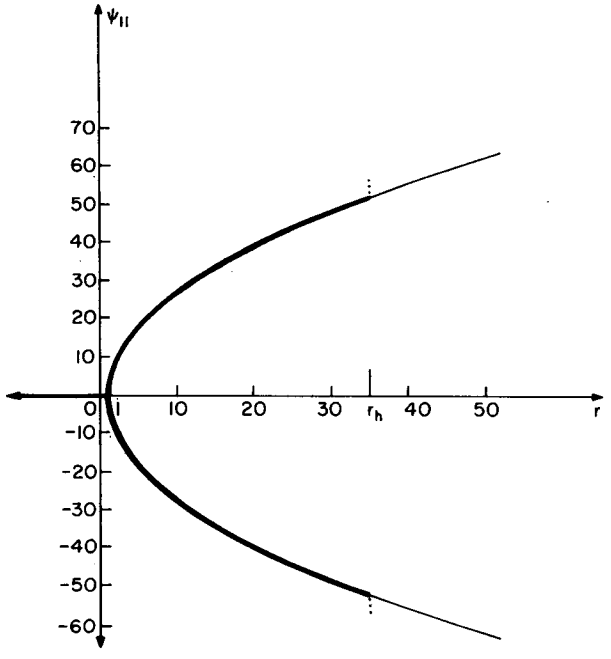

FIG. 2. A representation of the stationary solutions to the minimum model for the case Ha = 0 and $(A, \sigma) = (1, 10)$. Linearly stable solutions are denoted by the heavier lines, and a dotted line indicates the existence but not necessarily the exact location of a branching periodic solution. The trivial solution coincides with the r axis and exists for all values of r.

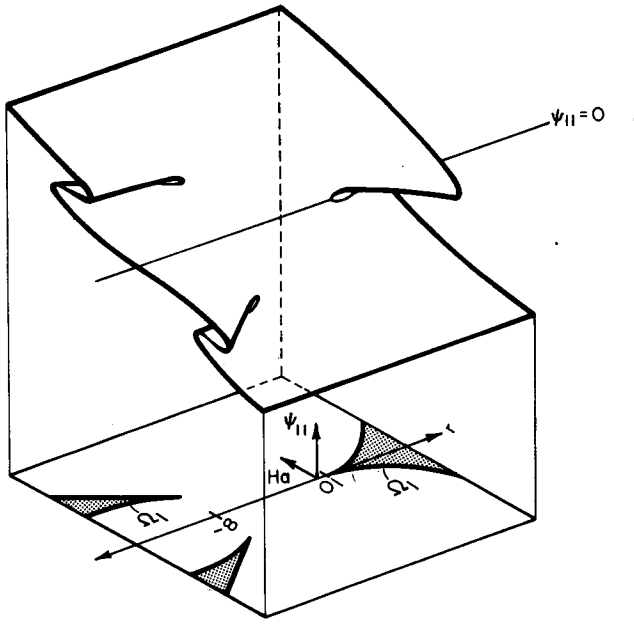

FIG. 3. A schematic diagram showing the relationship between the folded solution surface of (3.9)–(3.11) and the singularity set Ω_1 in the r-Ha plane. For values of r and Ha inside the cusps of Ω_1 (shaded regions), three distinct real roots of (3.14) exist, but for values of r and Ha outside Ω_1, only one real root exists.

that separates the values of Ra and Ha for which (3.14) admits of one or three real solutions is called the singularity set Ω_1 (Fig. 3). For values of Ra and Ha in Ω_1, Eq. (3.14) has either two or three coincident real roots which correspond to singular points of (3.9)–(3.11). In Fig. 3, this set appears as the cusps in the r-Ha plane below the solution surface.

We may obtain the entire singularity set Ω_1 of (3.9)–(3.11) by setting the discriminant D of the cubic equation (3.14) to zero (Uspensky, 1948). The values of h^2 that cause D to vanish are given by

$$h^2 = \{(r^2 - 20r - 8) + [r(r+8)^3]^{1/2}\}\lambda_{11}^4\lambda_{31}/16, \quad \text{for } r \geqslant 1 \text{ or } r \leqslant -8, \qquad (3.20)$$

or

$$h^2 = \{(r^2 - 20r - 8) - [r(r+8)^3]^{1/2}\}\lambda_{11}^4\lambda_{31}/16, \quad \text{for } r \leqslant -8, \qquad (3.21)$$

which together define the three cusps of Ω_1 in the r-Ha thermal parameter plane. We note that replacement of Ha by h causes the form of the singularity set Ω_1 to be independent of A or σ.

The three cusp points of Ω_1 in Fig. 3 correspond to triple roots of (3.14). The other points of Ω_1 are fold points at which two families of solutions coalesce. From Fig. 3 we see that the interiors of the cusps are the sets of values of r and Ha for which (3.14) has three distinct real solutions. Throughout the remainder of the thermal parameter plane (3.14) has only one real root.

Unauthenticated | Downloaded 12/06/21 03:22 AM UTC

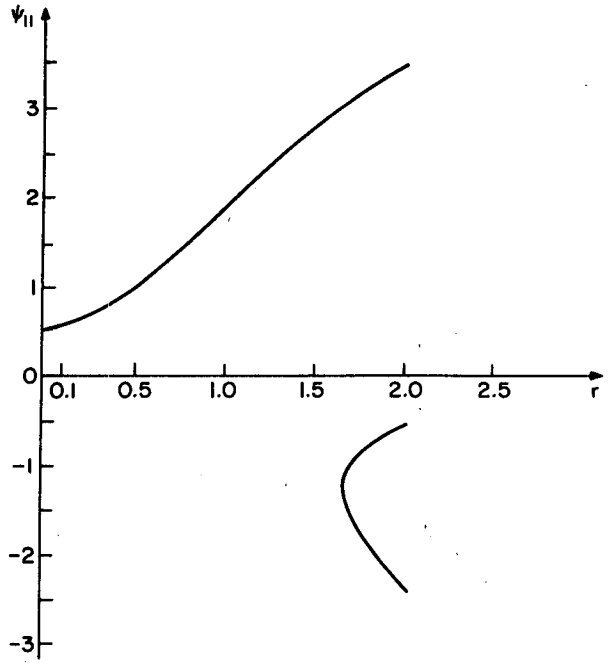

FIG. 4. A constant-Ha cross section through the steady solution surface of (3.9)–(3.11) for Ha = 1 and $(A, \sigma) = (0.1, 0.73)$. The qualitative behavior shown here is the same for any constant-Ha cross section depicting multiple solutions, except the one for Ha = 0, as in Fig. 2.

In Fig. 3 we also show the magnitudes of the component ψ_{11} of the steady states as functions of r and Ha. We choose ψ_{11} because its use does not distort the steady behavior that actually lies in a five-dimensional space, and because ψ_{11} entirely defines the velocity field. The resulting graph for $r > 0$ resembles the cusp surface discussed for catastrophe theory by Zeeman (1976) and Poston and Stewart (1978).

After comparing Figs. 2 and 3, we see that the bifurcation diagram obtained from the Lorenz (1963) model of primitive Rayleigh flow is actually a special case of the more general convective situation. If we examine any Ha $\neq 0$ cross section through the cusp surface of Fig. 3, then we see from Fig. 4 that the resulting distribution of ψ_{11} is qualitatively different from the singular behavior of the bifurcative case given in Fig. 2.

We expect that the developing convective solution will be manifested in a way not sensitive to specific choices of the values of parameters such as Ha; therefore, the behavior depicted in Fig. 4 is much more likely to occur than that shown in Fig. 2. Indeed, Tavantzis *et al.* (1978) state that careful experiments of Bénard convection show that stationary branching as depicted in Fig. 2 is not observed. Rather, the convective solution is described by the upper branch in Fig. 4. They noted that the observed flow plausibly can be ascribed to either thermal noise in the bounding plates—which in our model corresponds to Ha $\propto \Delta_y T \neq 0$—or to variations in the vertical distance between the plates.

Thus our proposed model (3.9)–(3.11) for generalized convection provides an improved prediction of laboratory fluid behavior. It is important to note that the deficiency of the original Lorenz (1963) model, whose branching diagram has the same form as that in Fig. 2, was not in the harmonic truncation to three equations, but in the choice of an incomplete set of control variables.

The two constant-r cross sections through the entire solution surface in Fig. 5 provide a different view of the steady states. When $r \leqslant 0$, only thermally direct stationary circulations (ψ_{11} Ha > 0) are possible, reflecting the fact that the fluid is statically stable (Fig. 5a). But from Fig. 5b we see that both thermally direct and indirect (ψ_{11} Ha < 0) flows may occur when $r > 0$. These last two possibilities are shown schematically in Fig. 1, in which for positive values of the horizontal heating (Ha < 0) a direct circulation corresponds to counterclockwise overturning fluid and an indirect flow to a clockwise circulation.

If we assume for the moment that all solutions depicted in Fig. 5 are linearly stable, then large or catastrophic changes in the observed steady state of the modeled system may occur for infinitesimal variations in the magnitude of Ha. For example, as the Hadley number Ha is decreased past the critical value near -60 in Fig. 5b, the indirect circulation ($\psi_{11} > 0$) disappears and the direct flow ($\psi_{11} < 0$) replaces it; this clearly corresponds to a significant change in the observed system (see Fig. 1).

Hysteresis can also occur in either statically stable or unstable fluids. For fixed values of Ha, we assume for the moment that the middle of three solutions is the only unstable one. In Fig. 5a we see that hysteresis within the direct circulation is possible because a transition will occur once |Ha| is increased past H_2 but will not occur until |Ha| is decreased past H_1.

In unstable stratification, however, hysteresis is manifested by a change in sign of the circulation. From Fig. 5b we see that once a clockwise circulation is established, the value of Ha can decrease to -60 before the counterclockwise overturning motion will replace it. But now the counterclockwise circulation can be maintained until Ha is increased past $+60$. Thus, both the observed sense of circulation and the critical value at which a transition from one type of cellular motion to the other depend on how the Hadley number is varied. These results will be refined in the following subsection, in which we find where the steady states can lose stability via Hopf bifurcation (at values of Ha that are in general different from those for the fold points). The prediction discussed above of hysteresis in horizontally forced convection, when refined with the stability analysis of the fol-

Unauthenticated | Downloaded 12/06/21 03:22 AM UTC

lowing subsection, could be examined in a laboratory experiment.

c. Stability

We will next ascertain which steady solutions of the minimum model are linearly stable and therefore likely to be observable. This can be determined from the real parts of the eigenvalues of the Jacobian matrix J obtained after linearization of (3.9)–(3.11) about a steady state (3.12)–(3.14) (Minorsky, 1962). The eigenvalues or characteristic exponents of J are the roots of the characteristic equation

$$\mu^3 + [(\sigma\lambda_{11} + \lambda_{31} + 4A^2)/A]\mu^2 + \left[0.5(1 + \sigma\lambda_{11}/\lambda_{31})\psi_{11}^2 - \frac{2A\,\mathrm{Ha}}{\lambda_{11}\lambda_{31}}\psi_{11} + \left(4\sigma\lambda_{11} + 4\lambda_{31} + \frac{\sigma}{A^2}\lambda_{11}\lambda_{31} - \frac{4\sigma\,\mathrm{Ra}'}{9\lambda_{11}}\right)\right]\mu + \left[1.5\frac{\lambda_{11}\sigma}{A}\psi_{11}^2 - \frac{4\,\mathrm{Ha}}{\lambda_{11}}\psi_{11} + \frac{4\lambda_{11}\lambda_{31}\sigma}{A}(1 - r)\right] = 0, \quad (3.22)$$

in which $\mathrm{Ra}' = 128\ \mathrm{Ra}\pi^{-4}$. We note from examination of (3.14) and (3.22) that the stability of the stationary solutions for a given value of Ha $\propto h$ is the same as the stability for $-$Ha because $\psi_{11}(-h) = \psi_{11}(h)$.

Because the coefficients of the characteristic equation (3.22) are real-valued, the characteristic exponents of a stationary solution will consist of either three real numbers or one real root and a complex conjugate pair of numbers. Therefore, in general, a family of stationary solutions to (3.9)–(3.11) may lose stability either by one real eigenvalue crossing through zero, which signals a steady bifurcation (Iooss, 1979), or via a complex conjugate pair of eigenvalues crossing the imaginary axis with nonzero speed, which corresponds to Hopf bifurcation (Marsden and McCracken, 1976).

It is easily shown that the fold or cusp points of the singularity set Ω_1 are the values of the parameters at which $\mu = 0$ in (3.22). Thus the only additional branching behavior in (3.9)–(3.11) occurs as Hopf bifurcations when $\mu = \pm i\alpha$. Indeed, because the minimum model reduces to one of Lorenz (1963) form for Ha = 0, we expect to find a line of values of r and h for which Hopf bifurcations occur whose value for Ha = 0 is $r = r_h$ (Fig. 2).

The characteristic exponents are roots of a cubic polynomial (3.22). It can be demonstrated easily that conjugate imaginary roots of the general cubic $x^3 + ax^2 + bx + c = 0$ occur if and only if $ab = c$ and $b \geq 0$; moreover, $x = \pm i\sqrt{b}$. Applying this result to (3.22), we find that Hopf bifurcation points are gov-

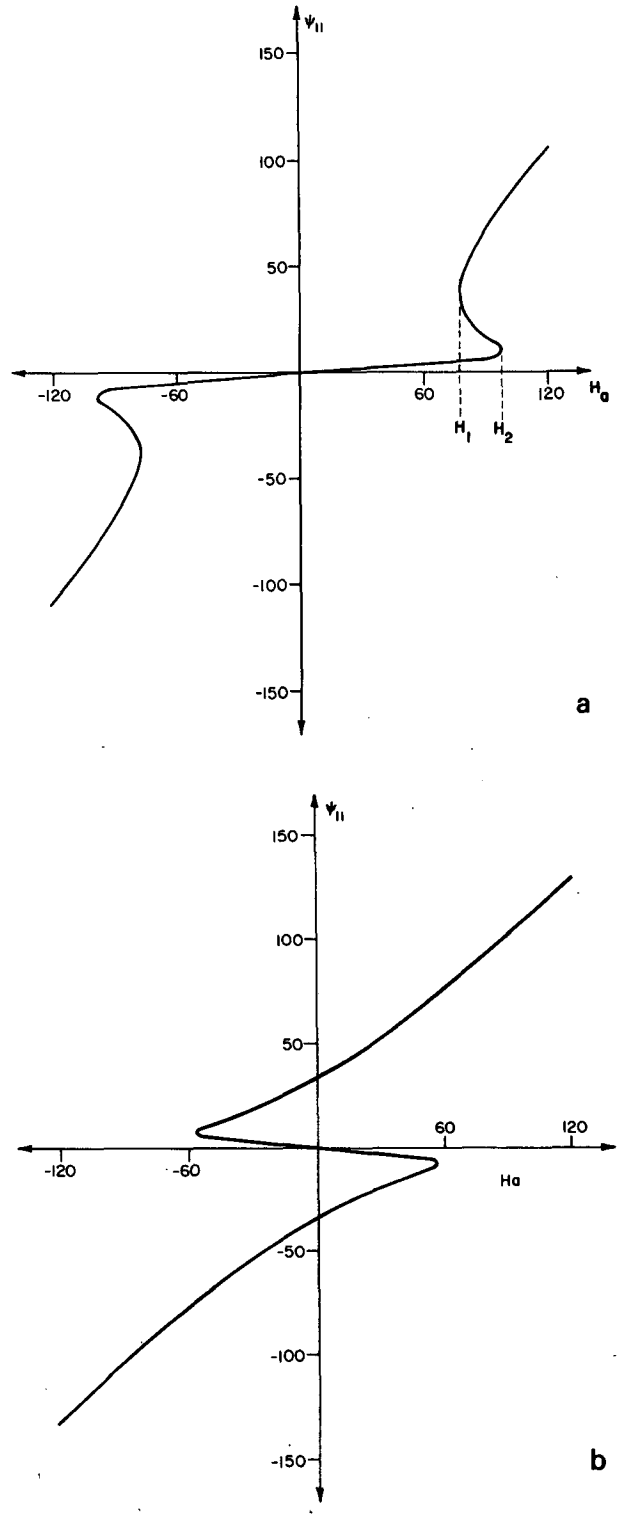

FIG. 5. Two constant-r cross sections through the stationary solution surface of the minimum model (3.9)–(3.11). Here (A, σ) = (1, 1), but the qualitative stationary solution behavior of the minimum model is independent of the particular choice of (A, σ). Here ψ_{11} Ha > 0 represents a thermally direct circulation, and ψ_{11} Ha < 0, a thermally indirect circulation. In (a) $r = -20$ and in (b) $r = 15$.

Unauthenticated | Downloaded 12/06/21 03:22 AM UTC

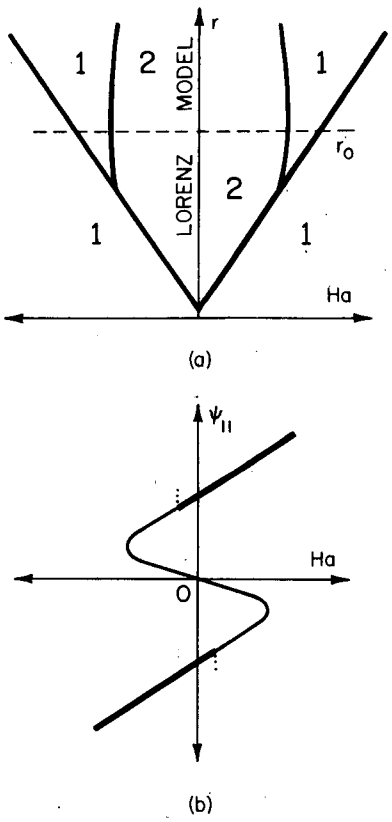

FIG. 6. The complete linear stability portrait for the steady solutions to the minimum model (3.9)–(3.11) when $r \geq 0$. In (a), a schematic representation of the Hopf bifurcation curves and part of the singularity set Ω_1 are given for $(A, \sigma) = (0.1; 1)$. The numbers refer to the number of stable stationary solutions in various regions of the thermal parameter plane. In (b), a schematic representation of the stationary solutions and their stability is shown for the $r = r_0$ cross section indicated in (a). Stable solutions are denoted by the heavier lines, and a dotted line indicates the existence but not necessarily the exact location of a branching periodic solution. Here both thermally direct (ψ_{11} Ha > 0) and thermally indirect (ψ_{11} Ha < 0) flows can be stable simultaneously.

erned by a quadratic equation in the variable h^2. The roots of this equation provide the three qualitatively distinct Hopf bifurcation curves depicted in Figs. 6–8. In these figures both the singularity set Ω_1 and the Hopf bifurcation curves are shown in the r-Ha plane together with a sketch of the steady-state behavior for each type of Hopf bifurcation curve. We do not show the portion of Ω_1 in the negative r half-plane because no Hopf bifurcations have been found for $r \leq 0$. The Ha = 0 axis is labelled "Lorenz model" because the resulting solutions come from a model of Lorenz (1963) type.

A general stability result is that the middle sheets of all the pleats represent unstable steady states (Figs. 6–8). Thus the stability characteristics of the cusp surfaces in the minimum model are in this respect similar to that of the cusp catastrophe surface (Poston and Stewart, 1978).

From Fig. 6b, we see that in the first case two stable stationary solutions exist simultaneously if r is sufficiently large in magnitude and Ha is sufficiently small. In this situation, both thermally direct and indirect flows are possible (Fig. 1). Fig. 6b shows that the stability exchange between a steady and a temporally periodic solution occurs only if the stationary state represents thermally indirect flow. Also, hysteresis is possible because the values of the Hopf bifurcation points are different for $\psi_{11} > 0$ and $\psi_{11} < 0$; however, we do not know whether or not the expected periodic solution is stable. The Hopf bifurcation curve obtained by Vickroy and Dutton (1979) in their three-component model of quasi-geostrophic flow is of the type shown in Fig. 6b.

The second class of Hopf bifurcation curves in Fig. 7b is distinguished by a self-intersection on the r axis at a value r_h of r. For $r > r_h$ and Ha sufficiently small in magnitude, all stationary solutions are unstable, and time-dependent flow is the only type observable. The point $(r_h, 0)$ corresponds to the Hopf bifurcation point in the Lorenz (1963) model. Lorenz found that Hopf bifurcation occurs only for some values of σ and a wavenumber-aspect ratio parameter; but by

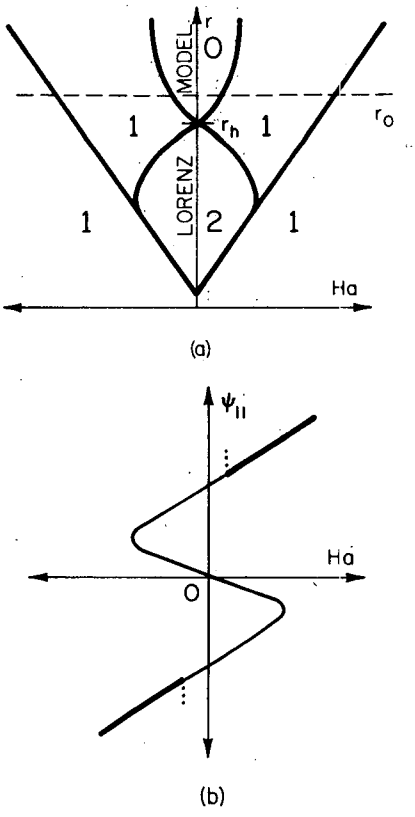

FIG. 7. As in Fig. 6 except that in (a) the representation is for $(A, \sigma) = (0.1, 4)$ and the Hopf bifurcation curves both cross the r axis at $r = r_h$. In (b) only thermally direct (ψ_{11} Ha > 0) flows can be stable.

Unauthenticated | Downloaded 12/06/21 03:22 AM UTC

comparing Figs. 6a and 7a, we see that the Hopf bifurcation curve in the r-Ha plane may simply fail to cross the r axis in this case. The existence of periodic solutions in two-dimensional convection is seen to occur for all values of A and σ when sufficient horizontal thermal forcing is included. Thus, we have a more complete description of the Hopf bifurcation than that available in the Lorenz (1963) model.

Fig. 8b exhibits the third kind of Hopf bifurcation curve. In this case, a one-parameter family of steady states loses but then regains stability via Hopf bifurcation as the value of Ha is varied. This behavior suggests that an entire family of periodic solutions exists that both emerges from and subsequently terminates on the stationary solution surface. This type of branching behavior occurred in the convection model of Shirer and Dutton (1979).

We also note that a catastrophe is likely when Ha is increased past a critical value Ha_f in Fig. 8b; but in order to prove this contention, a global stability analysis must be done. As discussed earlier, this catastrophic behavior would be manifested by a thermally direct steady flow suddenly and chaotically replacing a thermally indirect one upon a slight change in the value of Ha.

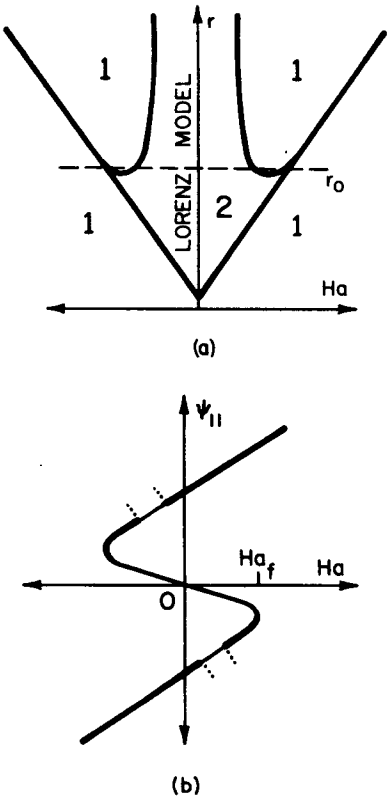

FIG. 8. As in Fig. 6 except that in (a) the representation is for $(A, \sigma) = (0.1, 0.73)$. In (b) both thermally direct (ψ_{11} Ha > 0) and thermally indirect (ψ_{11} Ha < 0) flows can be stable, but a thermally direct flow likely replaces the indirect one as Ha is increased past Ha_f.

4. Conclusion

In this article, we have developed a boundary-value problem to model two-dimensional flows of a fluid subject to externally imposed, time-independent horizontal and vertical temperature gradients. After the governing partial differential equations were nondimensionalized and the nondimensional boundary-value problem was spectrally decomposed, the resulting ordinary differential equations were spectrally truncated to obtain a three-component or minimum model. The resulting set is a generalized version of the form of the Lorenz (1963) model of Bénard or Rayleigh convection because horizontal heating, as measured by the Hadley number Ha, has been added to the vertical forcing given by the Rayleigh number Ra.

In the minimum model, it was found that both the number of and the distribution of the steady states are qualitatively independent of the aspect ratio (domain height over width) and the Prandtl number σ (ratio of the viscous and conductive coefficients). The singularity set, which is the collection of parameter values for which two or more stationary solutions meet, is described by three cusps in the thermal parameter plane. A family of the steady states may lose stability in one of two ways—either by branching to another time-independent solution or by Hopf bifurcation to a periodic solution.

The set of Hopf bifurcation points defines a pair of lines that emanate from the curves of the singularity set. The location of these Hopf bifurcation curves depends on both the aspect ratio A and the Prandtl number σ. In fact, three distinct types of Hopf bifurcation curves were identified. From this analysis it could be seen that Hopf bifurcation does not occur in a model of Lorenz (1963) type for some values of A or σ because the Hopf bifurcation curves fail to intersect the r axis.

The steady solutions may exhibit hysteresis and sudden change, or catastrophe. Mathematical catastrophe in the model corresponds to a small change in the magnitude of the horizontal forcing effecting either a large change in the average speed of the flow or even a transition from thermally indirect to thermally direct motion.

The minimum model has either one or three stationary solutions depending on the location of the thermal parameters Ra and Ha with respect to the singularity set. Without exception, unique steady solutions were found to be linearly stable. Moreover, the time-independent state is a global attractor in a neutrally stratified fluid (Ra = 0). For values of Ra, Ha and σ that typically represent statically unstable stratification and weak horizontal forcing in large Prandtl number fluids, all three steady states may

Unauthenticated | Downloaded 12/06/21 03:22 AM UTC

be unstable; in these cases, only time-dependent flows are observable.

The single most important implication of these minimum model results is that stationary solution bifurcation as found in the Lorenz (1963) model is not observable because this branching is achieved only when the magnitude of the horizontal forcing can be maintained exactly at zero, while the vertical forcing is increased. Physically this is improbable; moreover, Tavantzis *et al.* (1978) note that laboratory models of Bénard convection do not exhibit a transition of the type predicted by Lorenz's model as convection develops. An Ha $\neq 0$ cross section through the stationary solution surface of the minimum model closely resembles the observed branching behavior. Tavantzis *et al.* (1978) also attribute the observed transition to the presence of horizontal thermal inhomogeneities that correspond to Ha $\neq 0$ in the minimum model.

Thus, it is of paramount importance that a low-order spectral model contain the correct number of control parameters in order that all branching behavior near the most complicated singularity can be fully described and the singular behavior can be unveiled. For example, Shirer and Wells (1982) discuss a method for determining both the number and location of qualitatively significant parameters in a spectral system for values near a singular point. They demonstrate that the three-component model discussed here is complete in the above sense once the Hadley number is added to the Lorenz (1963) system.

The study of carefully designed, severely truncated spectral models should lead to a much improved understanding of the behavior in the more complete governing system because the observed flow is typically characterized by only a few spatial harmonics. Simply adding a parameter such as Ha allows physically realistic results to be obtained. As we have shown, it may be the parameter choice, not the truncation of basis functions, that is the limiting factor. This observation ultimately may lead to the development of relatively simple systems that can model apparently very complicated behavior.

Acknowledgments. We are deeply indebted to Professor John A. Dutton who suggested that we study the effects of horizontal heating. We are grateful for his advice and guidance that were freely provided to us during the preparation of this article. We also thank an anonymous reviewer whose questions and criticisms of the original manuscript allowed us to improve the content of the paper. The research reported here was partially funded by the National Science Foundation through Grants ATM 73-00662 and ATM 78-02699 and the National Aeronautics and Space Administration through Grant NSG-5347.

APPENDIX

Interaction Coefficients of the Spectral System (2.25)–(2.26)

To define the interaction coefficients, we introduce some notation. Let x be an algebraic expression and P be a logical expression. We then define

$$[x, P] = \begin{cases} x, & \text{if } P \text{ is true} \\ 0, & \text{if } P \text{ is false.} \end{cases}$$

In terms of this notation, the linear interaction coefficients are defined as

$$A_{pq} = [4/(pq),\ p \text{ and } q \text{ are odd}], \tag{A1}$$

$$B_{pjkq} = \left[\frac{4}{\pi^2} j\left(\frac{1}{p+j} + \frac{1}{p-j}\right)\left(\frac{1}{k+q} + \frac{1}{k-q}\right),\ p+j \text{ and } q+k \text{ are odd}\right], \tag{A2}$$

$$C_{pjqk} = \left[\frac{(4-2\delta_{k0})}{\pi^2} j\left(\frac{1}{p+j} + \frac{1}{p-j}\right)\left(\frac{1}{q+k} + \frac{1}{q-k}\right),\ p+j \text{ and } q+k \text{ are odd}\right], \tag{A3}$$

and the nonlinear interaction coefficients are defined as

$$\begin{aligned} 4D^{pq}_{mnrs} = {} & [nr - ms,\ r + m = p \text{ and } n + s = q] \\ & + [\mp(nr + ms),\ r - m = \pm p \text{ and } n + s = q] + [\mp(nr + ms),\ r + m = p \text{ and } n - s = \pm q] \\ & + [nr - ms,\ (r - m = p \text{ and } n - s = q) \text{ or } (r - m = -p \text{ and } n - s = -q)] \\ & + [-nr + ms,\ (r - m = p \text{ and } n - s = -q) \text{ or } (r - m = -p \text{ and } n - s = q)], \end{aligned} \tag{A4}$$

$$\begin{aligned} 4E^{pq}_{mnrs} = {} & [ms - nr,\ r + m = p \text{ and } s + n = q] \\ & + [\pm(ms + nr),\ r - m = \pm p \text{ and } s + n = q] + [-ms - nr,\ r + m = p \text{ and } s - n = \pm q] \\ & + [\mp(ms - nr),\ r - m = \pm p \text{ and } (s - n = q \text{ or } s - n = -q)]. \end{aligned} \tag{A5}$$

Unauthenticated | Downloaded 12/06/21 03:22 AM UTC

REFERENCES

Ahlers, G., and R. P. Behringer, 1978: Evolution of turbulence from the Rayleigh-Bénard instability. *Phys. Rev. Lett.*, **40,** 712–716.

Chandrasekhar, S., 1961: *Hydrodynamic and Hydromagnetic Stability.* Clarendon Press, 652 pp.

Charney, J. G., and J. G. Devore, 1979: Multiple flow equilibria in the atmosphere and blocking. *J. Atmos. Sci.*, **36,** 1205–1216.

Curry, J. H., 1978: A generalized Lorenz system. *Comm. Math. Phys.*, **60,** 193–204.

Dutton, J. A., 1976: *The Ceaseless Wind: An Introduction to the Theory of Atmospheric Motion.* McGraw-Hill, 579 pp.

——, and G. H. Fichtl, 1969: Approximate equations of motion for gases and liquids. *J. Atmos. Sci.*, **26,** 241–254.

Fenstermacher, P. R., H. L. Swinney, S. V. Benson and J. P. Gollub, 1979: Bifurcations to periodic, quasiperiodic, and chaotic regimes in rotating and convecting fluids. *Bifurcation Theory and Applications in Scientific Disciplines.* O. Gurel and O. E. Rössler, Eds., N.Y. Acad. Sci., 708 pp.

Fultz, D., R. R. Long, G. B. Owens, W. Boham, R. Kaylor and J. Weil, 1959: *Studies of Thermal Convection in a Rotating Cylinder with some Implications for Large-Scale Atmospheric Motions. Meteor. Monogr.*, No. 21, Amer. Meteor. Soc., 104 pp.

Hirsch, M. W., and S. Smale, 1974: *Differential Equations, Dynamical Systems, and Linear Algebra.* Academic Press, 358 pp.

Iooss, G., 1979: *Bifurcation of Maps and Applications.* North Holland, 232 pp.

Krishnamurti, R., 1970a: On the transition to turbulent convection, Part I. The transition from two- to three-dimensional flow. *J. Fluid Mech.*, **42,** 295–307.

——, 1970b: On the transition to turbulent convection, Part II. The transition to time-dependent flow. *J. Fluid Mech.*, **42,** 309–320.

Kuettner, J. P., 1959: The band structure of the atmosphere. *Tellus*, **11,** 267–294.

——, 1971: Cloud bands in the earth's atmosphere: Observations and theory. *Tellus*, **23,** 404–425.

Lorenz, E. N., 1960: Maximum simplification of the dynamic equations. *Tellus*, **12,** 243–254.

——, 1963: Deterministic nonperiodic flow. *J. Atmos. Sci.*, **20,** 130–141.

McLaughlin, J. B., and P. C. Martin, 1975: Transition to turbulence in a statically stressed fluid system. *Phys. Rev. A*, **12,** 186–203.

Marsden, J. E., and M. McCracken, 1976: *The Hopf Bifurcation and Its Applications. Applied Mathematical Sciences*, Vol. 19. Springer-Verlag, 408 pp.

Minorsky, N., 1962: *Nonlinear Oscillations.* Van Nostrand, 714 pp.,

Mitchell, K. E., and J. A. Dutton, 1981: Bifurcations from stationary to periodic solutions in a low-order model of forced, dissipative barotropic flow. *J. Atmos. Sci.*, **38,** 690–716.

Ogura, Y., and A. Yagihashi, 1970: A numerical study of finite-amplitude time-dependent convection induced by time-dependent internal heating: Truncated systems. *J. Meteor. Soc. Japan*, **48,** 1–17.

Poston, T., and I. Stewart, 1978: *Catastrophe Theory and Its Applications.* Pitman, 491 pp.

Shirer, H. N., 1980: Bifurcation and stability in a model of moist convection in a shearing environment. *J. Atmos. Sci.*, **37,** 1586–1602.

——, and J. A. Dutton, 1979: The branching hierarchy of multiple solutions in a model of moist convection. *J. Atmos. Sci.*, **36,** 1705–1721.

——, and R. Wells, 1982: Improving spectral models by unfolding their singularities. *J. Atmos. Sci.*, **39** (in press).

Tavantzis, J., E. L. Reiss and B. J. Matkowsky, 1978: On the smooth transition to convection. *SIAM J. Appl. Math.*, **34,** 322–337.

Uspensky, J. V., 1948: *Theory of Equations.* McGraw-Hill, 358 pp.

Vickroy, J. G., and J. A. Dutton, 1979: Bifurcation and catastrophe in a simple, forced, dissipative quasi-geostrophic flow. *J. Atmos. Sci.*, **36,** 42–52.

Zeeman, E. C., 1976: Catastrophe theory. *Sci. Amer.*, **234,** 65–83.

Unauthenticated | Downloaded 12/06/21 03:22 AM UTC